Molecular & Cellular Toxicology
https://doi.org/10.1007/s13273-024-00433-x

ORIGINAL ARTICLE

Induction of glioblastoma invasion triggered by system Xc⁻-mediated glutamate release

Jiyoon Baik[1] · Myunghoon Lee[1] · Jae Hong Yoo[1] · Ahyeon Jo[1] · Kyung-Seok Han[1]

Accepted: 22 January 2024

Abstract

Backgrounds Glioblastoma (GBM) is a highly aggressive brain cancer associated with poor prognosis, primarily attributed to its profound invasive characteristics. Glutamate is the main cause of invasion, and invasion is promoted by system Xc⁻ (cystine/glutamate antiporter), which is highly expressed in GBM. To date, no studies have examined the relationship between invasion and the specific downregulation of system Xc⁻ (xCT or *SLC7A11*) using shRNA in GBM.

Objective We aimed to determine the effect of a specific knockdown system, Xc⁻, in GBM using short hairpin RNA (shRNA) rather than pharmacological approaches.

Results Invasion was inhibited in GBM cells treated with sulfasalazine, a system Xc⁻ inhibitor. Our experiments validated a reduction in extracellular glutamate concentration following sulfasalazine treatment, without affecting GBM proliferation or calcium response. However, the efficacy of pharmacological methods is hindered by nonspecific effects and the prevalence of multiple side effects. Therefore, we specifically targeted the system Xc⁻ molecule through shRNA. Downregulation using shRNA demonstrated decreased invasion and extracellular glutamate levels, without affecting the calcium response and proliferation.

Conclusion The targeted inhibition of system Xc⁻ using shRNA yields a notable reduction in GBM invasion.

Keywords Glioblastoma · System Xc⁻ · Glutamate · Calcium · Invasion · Sulfasalazine · shRNA

Introduction

Glioblastoma (GBM) is the most aggressive and prevalent form of brain cancer originating from astrocytes. It is categorized as a World Health Organization grade IV tumor (Louis et al. 2021; Bleeker et al. 2012; Tan et al. 2020). GBM has a formidable invasion capacity, causes structural and functional damage to the brain (So et al. 2021), and has a poor prognosis (Tran and Rosenthal 2010). Even after surgical removal, temozolomide chemotherapy, and radiation treatment, the average survival time remains at 15 months (Grochans et al. 2022). In addition, even if surgical removal is performed, recurrence is inevitable due to pre-existing infiltration in other areas (Kang et al. 2010). Numerous factors contribute to GBM invasion, including cellular interactions with the matrix, intercellular junctions, and molecular signaling pathways (Stetler-Stevenson et al. 1993; Martin et al. 2013). Among these factors, studies have highlighted the significant roles of the extracellular matrix (ECM), calcium (Ca^{2+}), and glutamate signaling as the primary mechanisms regulating GBM invasion (So et al. 2021).

GBM upregulates the expression of various calcium signaling molecules, including G protein-coupled receptors (GPCR) and receptor tyrosine kinase (RTK) (So et al. 2021). Additionally, calcium moves from the extracellular space to the cytosol of GBM via store-operated channels (SOCs), Ca^{2+}-permeable transient receptor potential (TRP) channels, voltage-gated calcium channels (VGCCs), and $P2X_7$ receptors, leading to glioma invasion and migration (So et al. 2021). Calcium also enters into the GBM through the glutamate receptor α-amino-3-hydroxy-5-methyl-4-isoxazolepropionic acid (AMPA) and *N*-methyl-D-aspartate (NMDA) receptors (Radin and Tsirka 2020; Corsi et al. 2019). These two receptors are activated in the GBM by neuronal and glial paracrine glutamate (Lyons

Jiyoon Baik and Myunghoon Lee contributed equally to this work.

✉ Kyung-Seok Han
kshan711@cnu.ac.kr

[1] Department of Biological Science, Chungnam National University, Daejeon 34134, Republic of Korea

Published online: 07 March 2024

et al. 2007). Glutamate, the most important excitatory neurotransmitter involved in neuronal activity, promotes GBM migration, invasion, and proliferation (So et al. 2021). GBM releases glutamate instead of taking up it, thereby inducing the excitotoxic death of surrounding neurons and creating space for invasion (Ye and Sontheimer 1999; Chung et al. 2005; Sontheimer 2008; Noch and Khalili 2009). Additionally, GBM uses glutamate in an autocrine manner through the Xc-system, which is highly expressed in GBM (Lyons et al. 2007; Groot and Sontheimer 2011). Indeed, the release of glutamate from the GBM can trigger the activation of Ca^{2+}-permeable receptors such as AMPA or NMDA receptors. This activation leads to Ca^{2+} oscillations within the GBM cells or in neighboring GBM cells, subsequently facilitating the enhanced mobility of these cells. (So et al. 2021; Lyons et al. 2007).

System Xc^- (or xCT), encoded by the *SLC7A11* gene, serves as a cystine/glutamate transporter (Sato et al. 1999; Wang et al. 2003). The extracellular release of glutamate through the system Xc^- transporter leads to its binding to glutamate receptors, subsequently eliciting a Ca^{2+} response within the cell. System Xc^- is a protein composed of two chains, a specific light chain (xCT, *SLC7A11*) and a heavy chain, 4F2 (*SLC3A2*), connected by a disulfide bridge (Lewerenz et al. 2012). Sulfasalazine, a Food and Drug Administration-approved inhibitor of system Xc^-, is currently under active investigation for its potential application in glioma treatment (Bridges et al. 2012). A previous study showed that glioma invasion was reduced in the presence of sulfasalazine (Lyons et al. 2007). Furthermore, sulfasalazine serves as an inhibitor of sepiapterin reductase and displays antibacterial and anti-inflammatory effects (Costigan et al. 2012; Goldman and Peppercorn 1975). This multifaceted nature has led to its application in the treatment of inflammatory bowel disease (Nielsen 1982; Das 1989) including ulcerative colitis and Chron's disease (Sutherland et al. 1993; Klotz et al. 1980). Although the precise mechanism of action remains unclear, the reported side effects include depression, infertility, and immune thrombocytopenia (Cantarini et al. 2007). Therefore, in this study, we used a gene silencing method with shRNA rather than a pharmacological treatment.

Using the U-87 MG glioblastoma cell line, our initial experiments verified the reduction in glutamate release in cells treated with sulfasalazine. Subsequently, no significant variations were observed in the calcium response and proliferation compared with the control group. After generating and applying system Xc^--specific shRNAs, we observed a decrease in GBM cell invasion. Despite the observed reduction in invasion, no apparent differences were detected in terms of proliferation or calcium response. In summary, the targeted inhibition of system Xc^- in GBM effectively diminishes glutamate release, subsequently contributing to a reduction in the invasion.

Materials and methods

Cell culture

U-87 MG cells were purchased from ATCC (Manassas, VA, USA, #HTB-14). The cells were maintained in Dulbecco's Modified Eagle Medium (Corning, NY, USA, #10-013-CVRC) supplemented with 10% FBS (Gibco, NY, USA, #16000-044), and 1% penicillin–streptomycin solution (Cytiva, Seoul, Korea, #SV30010). All cells were grown at 37 °C in a humidified atmosphere containing 5% CO_2.

Glutamate assay

Extracellular glutamate concentrations were measured using a glutamate assay kit (Abcam, Cambridge, England, #ab83389). U-87 MG cells (1.0×10^6) were seeded on culture plates in under specified conditions, and the assay was conducted after 24 h of incubation. The cells were treated with 250 μM of sulfasalazine (Tocris, Bristol, England, #4935) 6 h after seeding and incubated for another 24 h. The media containing glutamate was harvested 24 h later. The harvested medium was centrifuged at 13,000 rpm for 1 min to remove cell debris, and only the supernatant was used. The concentration was calculated according to the manufacturer's instructions. The glutamate standard was prepared using 0.1 M glutamate and the assay buffer included in the kit. The standards were duplicated at concentrations of 0, 2, 4, 6, 8, and 10 nM. Both the standard and the sample were added to the well at 50 μL each, and the sample was diluted 1/10 and 1/20 in the assay buffer. 100 μL of reaction mix was added to every well, and the mix consisted of 90 μL of assay buffer, 8 μL of developer, and 2 μL of enzyme. After adding the mix, the sample was protected from light and reacted at 37 °C for 30 min. Absorbance was obtained by measuring OD450 nm. The concentration was calculated using the formula: $GlutamateConcentration = \left(\frac{Sa}{Sv}\right) * D$. (Sa = Amount of sample (nmol) from the standard curve, Sv = Volume of sample (μL) added into the well, D = Sample dilution factor.)

Calcium imaging

For calcium imaging, all cells were cultured at a uniform density on poly-D-lysine-coated (Sigma-Aldrich, MO, USA, #P6403) 12-mm Ø cover glasses (#0111520; Paul Marienfeld, Lauda-Königshofen, Germany). Groups subjected to 250 μM sulfasalazine treatment (Tocris, Bristol, England,

#4935) were incubated overnight. The external solution, designed for optimal imaging conditions, contained 150 mM NaCl (Sigma-Aldrich, MO, USA, #S9888), 10 mM HEPES (Carl Roth, Karlsruhe, Germany, #230-907-9), 3.2 mM KCl (Sigma-Aldrich, MO, USA, #P9541), 2 mM $CaCl_2$ (Sigma-Aldrich, MO, USA, #C3881), 2 mM $MgCl_2$ (Sigma-Aldrich, MO, USA, #M2670), 22 mM sucrose (Carl Roth, Karlsruhe, Germany, #200–334-9), and 5.6 mM glucose (Sigma-Aldrich, MO, USA, #G8270), and pH was adjusted to 7.4. All cells underwent a 40-min incubation in an external solution containing 5 μM Fura-2 AM (Invitrogen, MA, USA, #F1201) plus 1 μM pluronic acid (Sigma-Aldrich, MO, USA, #P2443). Imaging Workbench version 9.0.14.0 was used for the acquisition of intensity images and ratio calculations. The ligand TFLLR (synthesized by PEPTRON, Daejeon, Korea) was utilized in the study.

Proliferation assay

Cell proliferation was measured using a Quanti-Max WST-8 Cell Viability Assay Kit (BIOMAX, Guri, Korea, #QM1000). A seeding density of 1×10^5 U-87 MG cells was maintained on culture plates for each experimental condition. Following a 24 h incubation period, a proliferation assay was performed according to the manufacturer's instructions. OD 450 values were determined for the naïve or scrambled shRNA groups by randomly pairing naïve and sulfasalazine groups or scrambled shRNA and system Xc- shRNA groups into one set.

shRNA cloning

The Xc-shRNA oligo system was synthesized by Cosmo Genetech (Daejeon, Korea). The cloning process following the shRNA sequences was used for cloning: (Shin et al. 2017). pSicoR-mCh-empty (#21907; Addgene), XhoI (#R0146S; BioLabs), HpaI (#R0105S; BioLabs), rCutSmart (BioLabs, MA, USA, #B6004S) and LaboPass Gel, and a PCR Clean-up kit (Cosmo Genetech, Daejeon, Korea, #CMA0112) were used for vector digestion and elution. NEB buffer (BioLabs, MA, USA, #B7002S), T4 polynucleotide kinase (Enzynomics, Daejeon, Korea, #M005S), T4 polynucleotide kinase buffer (Enzynomics, Daejeon, Korea, #B305), ATP (Sigma, MO, USA, #A26209), T4 DNA ligase (Enzynomics, Daejeon, Korea, #M001S), and T4 DNA ligase buffer (Enzynomics, Daejeon, Korea, #B304) were used for shRNA oligo annealing, phosphorylation, and construct ligation. The ligation product was transformed using DH5α competent cells (Enzynomics, Daejeon, Korea, #CP011). LB Broth (LPS solution, Daejeon, Korea, #LB-05), Bacto Agar (Becton Dickinson, NJ, USA, #214010), and ampicillin (Cayman Chemical, MI, USA, #14417) were used for *E. coli* growth, and the LaboPass plasmid mini kit (Cosmo Genetech, Daejeon, Korea, #CMP0112) was used to extract the plasmids from *E. coli*. The shRNA sequence was confirmed using Cosmo Genetech (Daejeon, Korea).

Candidate 1 sense: 5′-GCTGAATTGGGAACAACT ATA-3′

Candidate 2 sense: 5′-GCAGTTGCTGGGCTGATT TAT-3′

Lentivirus production

The lentivirus was generated following the Addgene Lentiviral Guide. Transfection involved the introduction of 0.75 μg/mL psPAX2 (Addgene, MA, USA, #12260), 0.25 μg/mL pMD2.G (Addgene, MA, USA, #12259), and 1 μg/mL pSicoR-shRNA-mCh vector into HEK 293T cells using lipofectamine 3000 (Thermo Fisher Scientific, MA, USA, # L3000001). Opti-MEM (Gibco, NY, USA, #31985070) was used to ensure transfection efficiency, and HEK 293T cells were grown in an antibiotic-free medium. The packaging mix was injected into the HEK 293T cells at 80% density. Viruses were collected at 24-h intervals for 3 days. To enhance infection efficiency, polybrene (Merck Millipore, MA, USA, #TR-1003-G) was added at 1 μL/mL. The virus was aliquoted into 1 mL portions in cryotubes and stored at − 80 °C. Lentivirus cells were then introduced into U-87 MG at 20% density, and the medium was replaced 24 h later to promote cell growth and improve expression efficiency.

qRT-PCR

Total RNA was extracted 72 h after shRNA lentivirus infection using the RNeasy Mini Kit (QIAGEN, Hilden, Germany; #74106). RNA at 1,000 ng/μL per condition was synthesized into cDNA using SuperScript III First-Strand (Invitrogen, MA, USA, #18,080–051) and MiniAmp Thermal Cycler (Thermo Fisher Scientific, MA, USA, #A37834). qRT-PCR was performed using PowerSYBR Green PCR Master Mix (Applied Biosystems, MA, USA, #4367659) and a CFX96 Optics Module (Bio-Rad, CA, USA). Gene expression was normalized using the ΔΔCt method compared with the scrambled shRNA group. The primers used in the qRT reaction were as follows.

Human system Xc^- forward: 5′-CAAGGTGCCACTGTT CATCC-3′

Human system Xc^- reverse: 5′-CCACCTGGGTTTCTT GTCC-3′

Human GAPDH forward: 5′-GTCTCCTCTGACTTC AACAGCG-3′

Human GAPDH reverse: 5′-ACCACCCTGTTGCTGTAG CCAA-3′

Invasion assay

For each experimental condition, 1.0×10^5 U-87 MG cells were seeded on transwell plates (SPL, Pocheon, Korea, #35224) embedded with VitroGel hydrogel matrix (TheWell Bioscience, NJ, USA, #VHM01). The transwell chambers were filled with serum medium (2%), while 20% serum medium was placed outside the transwell chambers. Subsequently, the cells were incubated for 48 h. Treatment with 250 μM sulfasalazine (Tocris Bioscience, Bristol, England, #4935) was administered for 48 h. DPBS (WELGENE, Gyeongsan, Korea, #LB001-01), 3.7% formaldehyde (Sigma-Aldrich, MO, USA, #252549), methanol (Samchun Chemical Co., Ltd., Seoul, Korea, #M0588), and 4′,6-diamidino-2-phenylindole, dihydrochloride (DAPI) (Thermo Fisher Scientific, MA, USA, #62248) were used. The invaded areas were measured using ImageJ software (Ver. 1.53 k). Three images were randomly captured per well, and the average of the three regions was compared with the average of naïve cell wells. The data were expressed as the percentage of invasion.

Statistical data analysis

Photograph area analysis was conducted using Image J (Ver. 1.53 k). All bar graphs, trace figures, and statistical analyses were generated using GraphPad Prism (Ver. 9.4.1). For comparisons involving two subjects, a two-tailed unpaired Student's *t*-test was performed. For comparisons involving more than two subjects, a one-way analysis of variance was followed by a Dunnett's multiple comparisons test. All data were expressed as the mean with the standard error of the mean. $^{*}P < 0.05$, $^{**}P < 0.01$, $^{***}P < 0.001$, $^{****}P < 0.0001$, and ns were not considered significant.

Results

Sulfasalazine inhibiting glutamate release from U-87 MG

Previous studies have demonstrated the glioma-reducing properties of sulfasalazine (an inhibitor of system Xc^-) (Lyons et al. 2007). We also compared the amount of glutamate released from U-87 MG cells treated with sulfasalazine. The glutamate assay revealed a notable reduction in glutamate release in the sulfasalazine-treated group (Fig. 1A). This finding confirmed the inhibitory effect of sulfasalazine on system Xc^-, which decreases glutamate release from U-87 MG.

Calcium is a signaling molecule that influences the mobility and invasiveness of GBM (So et al. 2021). Therefore, calcium imaging was conducted to determine whether the GPCR pathway-related calcium response is affected by sulfasalazine (Fig. 1B). In this study, we used TFLLR to induce an activity-dependent calcium response, employing Fura 2-AM as a calcium indicator, as described previously (Roe et al. 1990). TFLLR functions as a selective peptide agonist that targets protease-activated receptor 1 (PAR1) (Hollenberg et al. 1997; Woo et al. 2012). PAR1, a member of the G protein-coupled receptor (GPCR) family, exhibits coupling with various G proteins such as $G_{\alpha i}$, $G_{\alpha q/11}$, and $G_{\alpha 12/13}$. Consequently, the presence of TFLLR triggers an intracellular calcium response due to this coupling. No significant difference was found in the intracellular calcium response between the sulfasalazine-treated and control groups (Fig. 1C and D). This finding suggests that glutamate release, which is reduced by sulfasalazine, does not affect GPCR-mediated intracellular calcium response in U-87 MG cells.

Decreased glutamate release in U-87 MG by silencing system Xc^-

Although sulfasalazine is a commonly used treatment for glioma, it is nonspecific to system Xc^- and has various side effects (Bridges et al. 2012; Cantarini et al. 2007). To address this, we used a short hairpin RNA (shRNA) to specifically silence system Xc. Figure 2A shows a schematic diagram of shRNA production and lentivirus infection. To validate the knockdown efficiency, qRT-PCR was performed in triplicate (Fig. 2B). Among the candidates, Candidate 1 exhibited superior knockdown efficiency, showing statistical significance Consequently, Candidate 1 was selected as the Xc-shRNA system for subsequent experiments.

Next, a glutamate assay was conducted to assess the knockdown effect achieved by the application of shRNA. The results revealed a significant reduction in glutamate release within the system Xc-shRNA group compared with that in the scrambled shRNA group (Fig. 3A). Additionally, calcium imaging using TFLLR was performed to determine whether the intracellular calcium response was altered by the introduction of Xc-shRNA (Fig. 3B). No difference was found in the calcium response between the scrambled shRNA and Xc-shRNA groups (Fig. 3C and D). These collective findings indicate that glutamate release is reduced in U-87 MG cells by the application system Xc-shRNA and is not related to the GPCR-mediated intracellular calcium response.

Regulation of U-87 MG invasion influence by glutamate released by system Xc^-

To determine the impact of reduced glutamate release resulting from *SLC7A11* gene silencing on the invasion of GBM cells, an invasion assay was performed. Compared with the

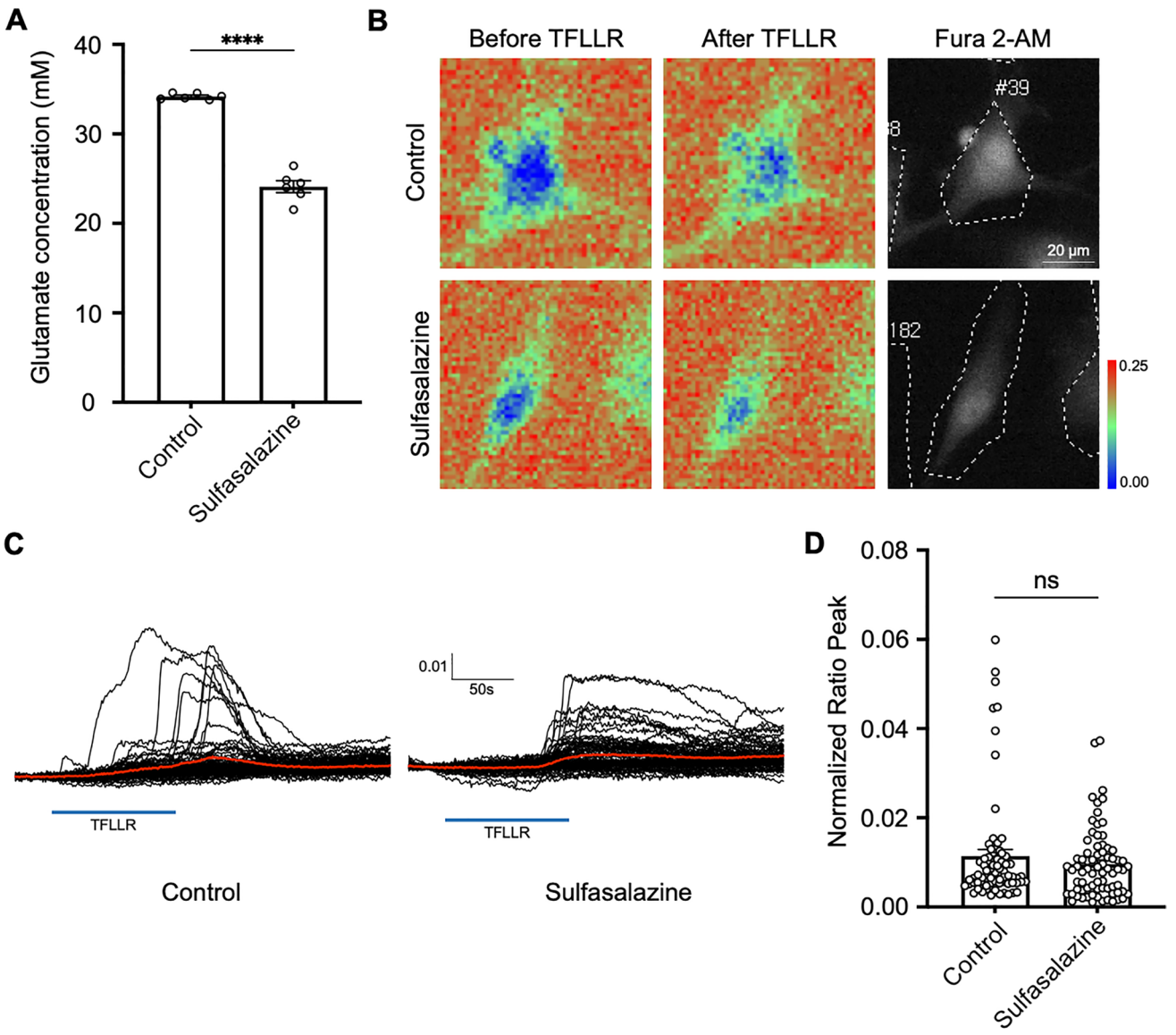

Fig. 1 Sulfasalazine reduces glutamate release independent of calcium response. **A** The bar graph shows the concentration of glutamate in each condition (n = 6, respectively). The individual dot indicates the data from a single well. **B** The images for calcium imaging from U-87 MG loaded with Fura 2-AM. Scale bar = 20 μm. The scale bar on the right represents the normalized 340/380 nm ratio. **C** Traces of calcium imaging from control cells (left, n = 73) and cells treated with 250 μM sulfasalazine (right, n = 74). Scale bars = 0.01 ratio, 50 s time. The black trace depicts the calcium signal for individual cells, while the red trace represents the average value of the cells. The blue horizontal bar denotes the application of 30 μM TFLLR at the indicated time. **D** The bar graph illustrates the normalized 340/380 nm peak. Each dot represents the data from a single cell. All data are expressed as the mean with standard error of the mean. All data were analyzed by two-tailed unpaired Student's *t*-test. $^{****}P < 0.0001$

scrambled shRNA group, the Xc-shRNA-expressing group showed a significant reduction in invasion (Fig. 4A and B). The invasiveness index, calculated as the percentage of shRNA-expressing cells ($mCherry^+$) relative to the total number of invading cells ($DAPI^+$), demonstrated a notable decrease from 77.9% in the scrambled shRNA group to 9.7% in the Xc-shRNA group.

An additional proliferation test was conducted; however, no significant differences were observed between the experimental groups. (Fig. 4C). These findings indicate that the glutamate released by system Xc^- does not significantly influence the proliferation of GBM but specifically affects its invasive capacity. Moreover, it demonstrated a similar effect to sulfasalazine treatment on invasion, proliferation, and calcium response, implying its potential as an alternative to sulfasalazine for the treatment of GBM.

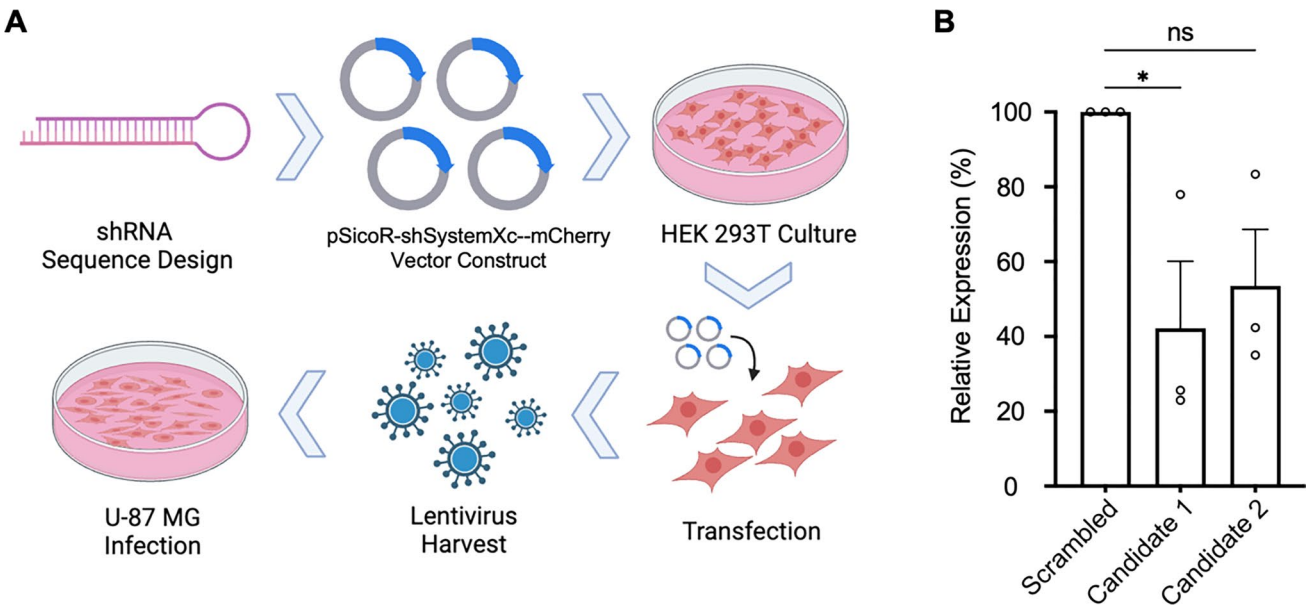

Fig. 2 Knockdown of *SLC7A11* in U-87 MG by shRNA. **A** Schematic image of the procedure of shRNA production and lentiviral infection. **B** Bar graph depicting the relative expression in each condition (n = 3, respectively). Each dot represents the data from a single tube, randomly paired and calculated. Data are expressed as the mean with standard error of the mean. All data were analyzed using one-way analysis of variance followed by Dunnett's multiple comparisons test. $^{*}P < 0.05$

Discussion

Figure 5 presents a schematic summary of the findings of this study. Both the pharmacological approach using sulfasalazine and the gene-silencing method using shRNA demonstrated efficacy in inhibiting glutamate release from U-87 MG cells. In alignment with the results of previous studies using sulfasalazine (Lyons et al. 2007), the inhibition of system Xc^- by shRNA reduced the invasion of GBM cells. Furthermore, the activation of $G_{\alpha q/11}$ using TFLLR showed no difference in calcium response among all experimental groups. This observation suggests that the autocrine signaling of glutamate through system Xc^- in GBM is more closely associated with the AMPA or NMDA receptor than with the GPCR pathway.

Glutamate plays a key role in the invasion process of glioblastoma (So et al. 2021; Lyons et al. 2007; Groot and Sontheimer 2011). Recent studies have highlighted the significance of ion movement mediated by AMPA or NMDA receptors in GBM, suggesting these receptors as potential therapeutic targets (Corsi et al. 2019; Nandakumar et al. 2019). Notably, the inhibition of AMPA receptors in GBM induces apoptosis (Ishiuchi et al. 2002). However, the role of NMDA receptors remains controversial. Some studies suggested their absence in glioma cells (Lyons et al. 2007; Stepulak et al. 2009), while others indicated that inhibiting NMDA receptors through antagonists reduces invasion (Nandakumar et al. 2019; Müller-Längle et al. 2019). Therefore, targeting AMPA or NMDA receptors has traditionally been considered for GBM treatment; however, the complexity of the signaling pathways involved poses challenges to the development of effective treatment strategies (Corsi et al. 2019; Ishiuchi et al. 2007). Beyond these receptors, the kynurenic acid receptor has also been identified as a regulator of GBM mobility (Walczak et al. 2014). Furthermore, the metabotropic glutamate receptor (mGluR) family in GBM warrants attention, given the limited research conducted on this aspect.

System Xc^- facilitates both glutamate export and cystine import. The physiological role of cysteine in cells is important. A study conducted a few years ago revealed that cystine uptake via system Xc^- triggered cell death under glucose-deprived conditions (Goji et al. 2017). Additionally, another study suggested that excessive cysteine absorption may lead to a phenomenon known as disulfidoptosis in GBM (Yan et al. 2023). Consequently, system Xc^- is intricately linked to both the glutamate and cystine metabolic pathways, making it challenging to draw definitive conclusions. Further research is required to fully elucidate their physiological functions.

This study used sulfasalazine to pharmacologically inhibit system Xc^-. Sulfasalazine is commonly utilized for the treatment of rheumatoid arthritis, ulcerative colitis, and Crohn's disease. It was approved for medical use in the United States in 1950 (Case 2001; Stuart et al. 2009; Pearl et al. 1986). It is mainly used to treat idiopathic urticaria, psoriasis, cirrhosis, and amyloidosis (McGirt et al. 2006; Gupta et al. 1990; Oakley et al. 2005; Brumshtein et al. 2015). Recently, it has been

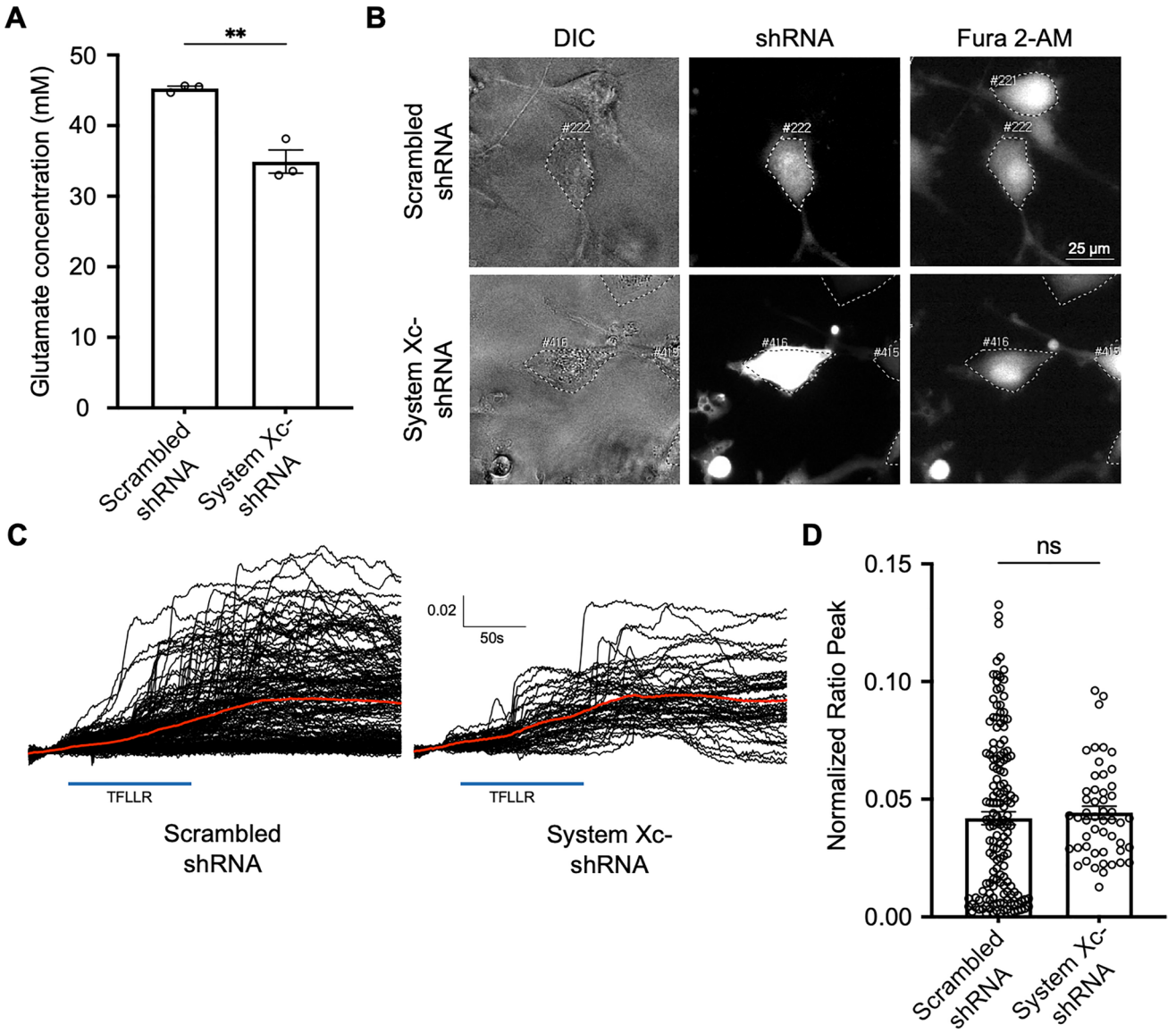

Fig. 3 System Xc^- knockdown by shRNA reduces glutamate release independent of calcium response. **A** The bar graph shows the concentration of glutamate in each condition (n = 3, respectively). Each dot represents the data from a single well. **B** Representative images of DIC, RFP, and Fura 2-AM from the left. Scale bar = 25 µm. **C** Calcium imaging traces from the from cells expressing scrambled shRNA (left, n = 153) and system Xc- shRNA (right, n = 51). Scale bars = 0.02 ratio, 50 s time. The black trace represents the calcium signal for individual cells, while the red trace denotes the average value of the cells. The blue horizontal bar indicates the application of 30 µM TFLLR at the specified time. **D** The bar graph shows the normalized 340/380 nm peak. Each dot represents the data from a single cell. All data are expressed as the mean with standard error of the mean. All data were analyzed by two-tailed unpaired Student's *t*-test. $^{**}P = 0.0034$

used in the treatment of pancreatic cancer, small cell lung cancer, and prostate cancer therapy (Lo et al. 2010; Guan et al. 2009; Doxsee et al. 2007), with ongoing investigations into its therapeutic viability for GBM (Bridges et al. 2012; Sontheimer and Bridges 2012). However, approximately 20–25% of patients using the medication have reported side effects (Stuart et al. 2009; Das et al. 1973). Symptoms such as nausea, vomiting, malaise, headache, and hemolysis are prevalent. The incidence of relatively mild side effects mainly depends on the dose used. Less frequent but more severe side effects that can affect almost any organ system have also been reported. These conditions include rashes, fever, joint pain, blood abnormalities, hepatitis, pneumonia, and male infertility (Peppercorn 1984). Hence, our findings suggest that employing gene-silencing methods might offer more promising avenues than conventional pharmacological drugs for targeting specific pathways or mechanisms of disease intervention. The potential expression of GBM-specific

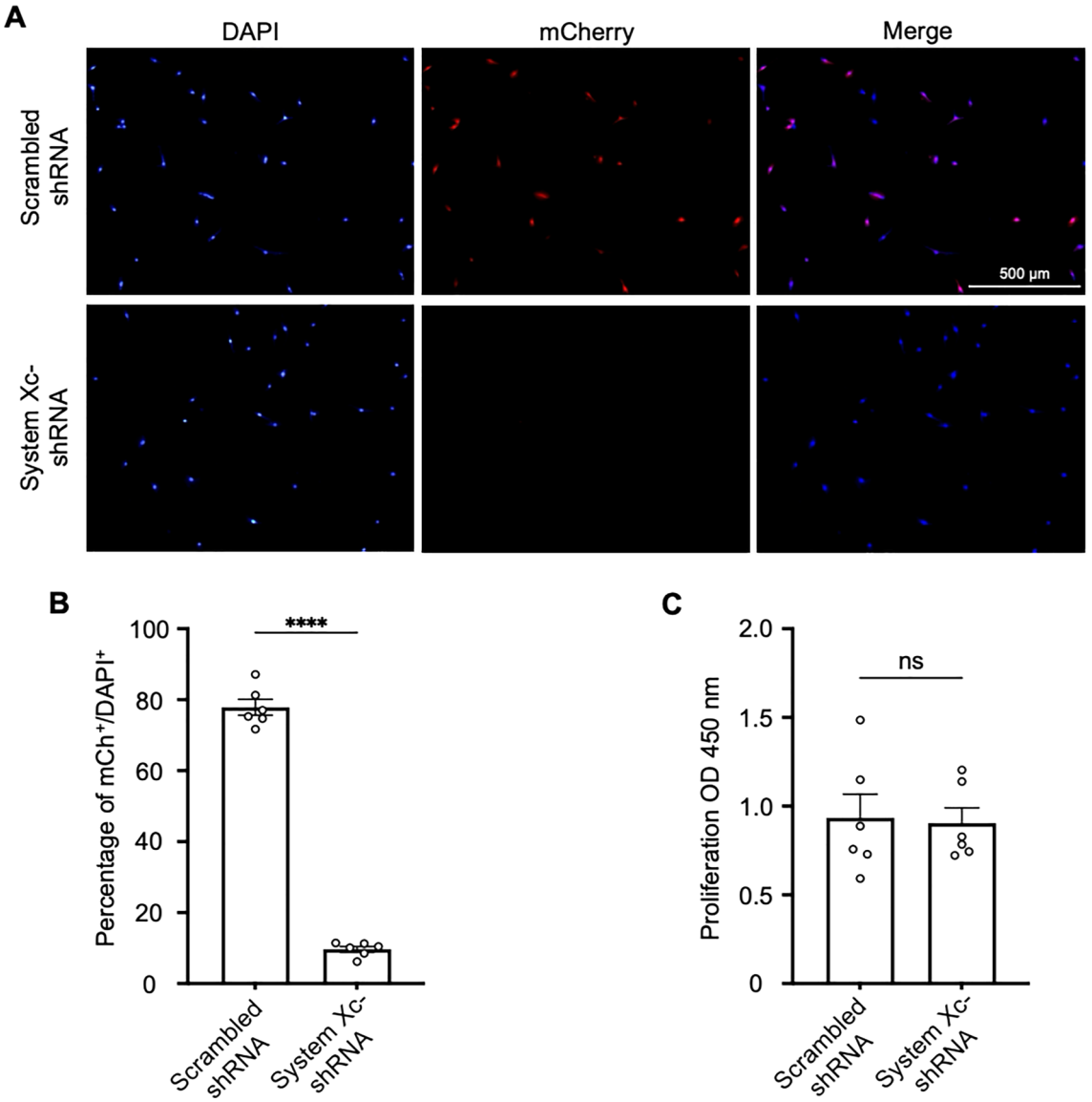

Fig. 4 Inhibition of system Xc^- via shRNA reduces the invasion of U-87 MG. **A** The representative images for the invasion assay were obtained by staining U-87 MG with DAPI in each expression condition. Scale bar = 500 µm. **B** The percentage of shRNA expression/DAPI stained cells was presented in each condition (n = 6, respectively). **C** The bar graph shows the proliferation O.D. values (n = 6, respectively). Each dot represents the data from a single well. All data are expressed as the mean with standard error of the mean. All data were analyzed using two-tailed unpaired Student's *t*-test. $^{****}P < 0.0001$

shRNAs holds promise, suggesting that achieving an ideal treatment for GBM might be attainable, provided that such targeted approaches can be effectively harnessed.

Finally, the implications of these studies should be extended to the treatment of human GBM. Therefore, validating the inhibition of invasion in an in vivo model or in patient-derived GBM samples is imperative. Based on our hypothesis, we anticipated reduced invasion and prolonged survival in the Xc knockdown group in GBM xenografts performed on nude mice. In addition, parallel in vitro experiments should corroborate decreased glutamate release and invasion of GBM samples obtained from patients. Although research on system Xc^- currently presents various possibilities and lacks clarity, further investigations to unravel its physiological functions could potentially open up promising avenues for GBM treatment.

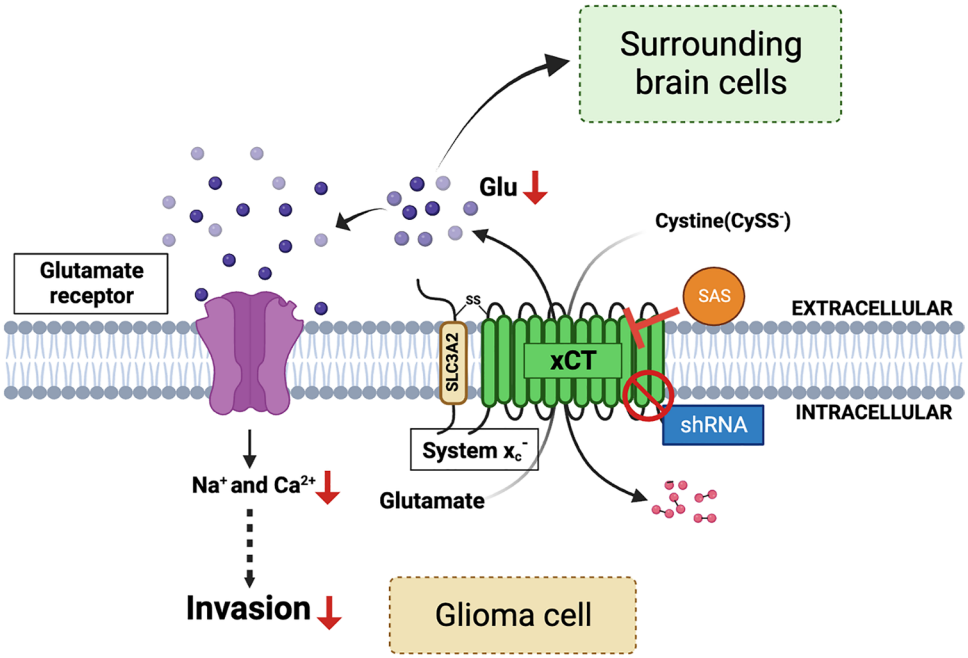

Fig. 5 Schematic diagram of the study process

Acknowledgements This work was supported by the Research Fund of the Chungnam National University. We would like to thank Editage (www.editage.co.kr) for English language editing.

Author contributions JYB conceived and designed the experiments. JYB and MHL wrote the manuscript. MHL and JHY designed and verified the experiments. AHJ conducted the qRT-PCR and invasion assays. KSH conceptualized the study and visualization and provided supervision. All authors discussed the data and reviewed the manuscript. All authors have read and approved the final version of the manuscript.

Data availability The datasets used during the current study are available from the corresponding author on reasonable request.

Declarations

Conflict of interest Jiyoon Baik declares that she has no conflicts of interest. Myunghoon Lee declares that he has no conflicts of interest. Jae Hong Yoo declares that he has no conflicts of interest. Ahyeon Jo declares that she has no conflicts of interest. Kyung-Seok Han declares that he has no conflicts of interest.

Ethical approval This article does not involve any studies with human participants or animals performed by any of the authors.

References

Bleeker FE, Molenaar RJ, Leenstra S (2012) Recent advances in the molecular understanding of glioblastoma. J Neurooncol 108:11–27

Bridges R, Lutgen V, Lobner D, Baker DA (2012) Thinking outside the cleft to understand synaptic activity: contribution of the cystine-glutamate antiporter (system xc−) to normal and pathological glutamatergic signaling. Pharmacol Rev 64:780–802

Brumshtein B et al (2015) Inhibition by small-molecule ligands of formation of amyloid fibrils of an immunoglobulin light chain variable domain. Elife 4:e10935

Cantarini L, Tinazzi I, Biasi D, Fioravanti A, Galeazzi M (2007) Sulfasalazine-induced immune thrombocytopenia. Postgrad Med J 83:e1–e1

Case JP (2001) Old and new drugs used in rheumatoid arthritis: a historical perspective: part 1: the older drugs. Am J Ther 8:123–143

Chung WJ et al (2005) Inhibition of cystine uptake disrupts the growth of primary brain tumors. J Neurosci 25:7101–7110

Corsi L, Mescola A, Alessandrini A (2019) Glutamate receptors and glioblastoma multiforme: an old "Route" for new perspectives. Int J Mol Sci 20:1796

Costigan M, Latremoliere A, Woolf CJ (2012) Analgesia by inhibiting tetrahydrobiopterin synthesis. Curr Opin Pharmacol 12:92–99

Das KM (1989) Sulfasalazine therapy in inflammatory bowel disease. Gastroenterol Clin North Am 18:1–20

Das K, Eastwood M, McManus J, Sircus W (1973) Adverse reactions during salicylazosulfapyridine therapy and the relation with drug metabolism and acetylator phenotype. N Engl J Med 289:491–495

de Groot J, Sontheimer H (2011) Glutamate and the biology of gliomas. Glia 59:1181–1189

Doxsee DW et al (2007) Sulfasalazine-induced cystine starvation: potential use for prostate cancer therapy. Prostate 67:162–171
Goji T, Takahara K, Negishi M, Katoh H (2017) Cystine uptake through the cystine/glutamate antiporter xCT triggers glioblastoma cell death under glucose deprivation. J Biol Chem 292:19721–19732
Goldman P, Peppercorn MA (1975) Sulfasalazine. N Engl J Med 293:20–23
Grochans S et al (2022) Epidemiology of glioblastoma multiforme–literature review. Cancers 14:2412
Guan J et al (2009) The xc− cystine/glutamate antiporter as a potential therapeutic target for small-cell lung cancer: use of sulfasalazine. Cancer Chemother Pharmacol 64:463–472
Gupta AK et al (1990) Sulfasalazine improves psoriasis: a double-blind analysis. Arch Dermatol 126:487–493
Hollenberg MD, Saifeddine M, Al-Ani B, Kawabata A (1997) Proteinase-activated receptors: structural requirements for activity, receptor cross-reactivity, and receptor selectivity of receptor-activating peptides. Can J Physiol Pharmacol 75:832–841
Ishiuchi S et al (2002) Blockage of Ca2+-permeable AMPA receptors suppresses migration and induces apoptosis in human glioblastoma cells. Nat Med 8:971–978
Ishiuchi S et al (2007) Ca2+-permeable AMPA receptors regulate growth of human glioblastoma via Akt activation. J Neurosci 27:7987–8001
Kang SS et al (2010) Caffeine-mediated inhibition of calcium release channel inositol 1, 4, 5-trisphosphate receptor subtype 3 blocks glioblastoma invasion and extends survival. Can Res 70:1173–1183
Klotz U, Maier K, Fischer C, Heinkel K (1980) Therapeutic efficacy of sulfasalazine and its metabolites in patients with ulcerative colitis and Crohn's disease. N Engl J Med 303:1499–1502
Lewerenz J, Maher P, Methner A (2012) Regulation of xCT expression and system function in neuronal cells. Amino Acids 42:171–179
Lo M, Ling V, Low C, Wang Y, Gout P (2010) Potential use of the anti-inflammatory drug, sulfasalazine, for targeted therapy of pancreatic cancer. Curr Oncol 17:9–16
Louis DN et al (2021) The 2021 WHO classification of tumors of the central nervous system: a summary. Neuro Oncol 23:1231–1251
Lyons SA, Chung WJ, Weaver AK, Ogunrinu T, Sontheimer H (2007) Autocrine glutamate signaling promotes glioma cell invasion. Can Res 67:9463–9471
Martin TA, Ye L, Sanders AJ, Lane J, Jiang WG (2013) Cancer invasion and metastasis: molecular and cellular perspective. In: Madame Curie bioscience database. Landes Bioscience, Austin
McGirt LY, Vasagar K, Gober LM, Saini SS, Beck LA (2006) Successful treatment of recalcitrant chronic idiopathic urticaria with sulfasalazine. Arch Dermatol 142:1337–1342
Müller-Längle A et al (2019) NMDA receptor-mediated signaling pathways enhance radiation resistance, survival and migration in glioblastoma cells—a potential target for adjuvant radiotherapy. Cancers 11:503
Nandakumar D, Ramaswamy P, Prasad C, Srinivas D, Goswami K (2019) Glioblastoma invasion and NMDA receptors: a novel prospect. Physiology Int 106:250–260
Nielsen O (1982) Sulfasalazine intolerance: a retrospective survey of the reasons for discontinuing treatment with sulfasalazine in patients with chronic inflammatory bowel disease. Scand J Gastroenterol 17:389–393
Noch E, Khalili K (2009) Molecular mechanisms of necrosis in glioblastoma: the role of glutamate excitotoxicity. Cancer Biol Ther 8:1791–1797
Oakley F et al (2005) Inhibition of inhibitor of κB kinases stimulates hepatic stellate cell apoptosis and accelerated recovery from rat liver fibrosis. Gastroenterology 128:108–120
Pearl RK, Nelson RL, Prasad ML, Orsay CP, Abcarian H (1986) Serious complications of sulfasalazine. Dis Colon Rectum 29:201–202
Peppercorn MA (1984) Sulfasalazine: pharmacology, clinical use, toxicity, and related new drug development. Ann Intern Med 101:377–386
Radin DP, Tsirka SE (2020) Interactions between tumor cells, neurons, and microglia in the glioma microenvironment. Int J Mol Sci 21:8476
Roe M, Lemasters J, Herman B (1990) Assessment of Fura-2 for measurements of cytosolic free calcium. Cell Calcium 11:63–73
Sato H, Tamba M, Ishii T, Bannai S (1999) Cloning and expression of a plasma membrane cystine/glutamate exchange transporter composed of two distinct proteins. J Biol Chem 274:11455–11458
Shin C-S et al (2017) The glutamate/cystine xCT antiporter antagonizes glutamine metabolism and reduces nutrient flexibility. Nat Commun 8:15074
So J-S, Kim H, Han K-S (2021) Mechanisms of invasion in glioblastoma: extracellular matrix, Ca2+ signaling, and glutamate. Front Cell Neurosci 15:663092
Sontheimer H (2008) A role for glutamate in growth and invasion of primary brain tumors. J Neurochem 105:287–295
Sontheimer H, Bridges RJ (2012) Sulfasalazine for brain cancer fits. Expert Opin Investig Drugs 21:575–578
Stepulak A et al (2009) Expression of glutamate receptor subunits in human cancers. Histochem Cell Biol 132:435–445
Stetler-Stevenson WG, Aznavoorian S, Liotta LA (1993) Tumor cell interactions with the extracellular matrix during invasion and metastasis. Annu Rev Cell Biol 9:541–573
Stuart MC, Kouimtzi M, Hill S (eds) (2009) WHO model formulary 2008. World Health Organization
Sutherland LR, May GR, Shaffer EA (1993) Sulfasalazine revisited: a meta-analysis of 5-aminosalicylic acid in the treatment of ulcerative colitis. Ann Intern Med 118:540–549
Tan AC et al (2020) Management of glioblastoma: State of the art and future directions. Cancer J Clin 70:299–312
Tran B, Rosenthal M (2010) Survival comparison between glioblastoma multiforme and other incurable cancers. J Clin Neurosci 17:417–421
Walczak K et al (2014) Kynurenic acid inhibits proliferation and migration of human glioblastoma T98G cells. Pharmacol Rep 66:130–136
Wang H et al (2003) Expression of the activity of cystine/glutamate exchange transporter, system xc−, by xCT and rBAT. Biochem Biophys Res Commun 305:611–618
Woo DH et al (2012) TREK-1 and Best1 channels mediate fast and slow glutamate release in astrocytes upon GPCR activation. Cell 151:25–40
Yan Y et al (2023) SLC7A11 expression level dictates differential responses to oxidative stress in cancer cells. Nat Commun 14:3673
Ye Z-C, Sontheimer H (1999) Glioma cells release excitotoxic concentrations of glutamate. Can Res 59:4383–4391